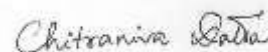


DECLARATION

I, **Chitraniva Datta** bearing Ph.D. Registration Number, **Ph.D./1770/2011 dt. 22.09.11** hereby declare that the thesis entitled “**Synthesis, Photoluminescence and Mesogenic Properties of Some d- and f-block Metal Schiff Base Complexes**” submitted to Assam University, Silchar for the partial fulfillment of the degree of Doctor of Philosophy in Chemistry is the record of work done by me under the supervision of Prof. C. R. Bhattacharjee, Department of Chemistry, Assam University, Silchar. I further declare that the contents of this thesis have not formed the basis for the award of any other degree/diploma.



Place: Assam University, Silchar

(Chitraniva Datta)

Date: 24.04.2015

Dedicated to my parents

Sri Panna Lal Datta

&

Smt. Sumita Datta

Acknowledgement

In the beginning, I pay homage to Almighty for blessings bestowed on me to complete this research work.

With great demureness, I am grateful to my Supervisor, Prof. C. R. Bhattacharjee, Department, of Chemistry, Assam University, Silchar, Assam for giving me the opportunity to work with him, for the constructive discussions and for supervising my work with attention. Working under him has been a rich and rewarding experience. I am very much indebted to him for his guidance, invaluable suggestions and for everything that I could learn from him.

I am thankful to Prof. B. S. Purkayastha, Dean, Albert Einstein School of Physical Sciences, Assam University, for his sustained support.

I sincerely thank Dr. P.C. Paul, Associate Professor, Department of Chemistry, for the constant inspiration and effective suggestions throughout my research tenure.

I owe a special note of gratitude to our collaborator, Dr. P. Mondal, Department of Chemistry, for computational analysis.

I would like to thank Dr. Sk. Jasimuddin, Department of Chemistry, for carrying out cyclovoltammetric measurements.

I wish to thank Prof. S. B. Paul, Dr. M. K. Paul, Dr. D. Sengupta, Dr. H. Acharya, Dr. S. K. Ghosh, Dr. S. Choudhury, Dr. T. S. Singh and Dr. R. Panchadhayee, faculty members of the Department for providing all sorts of support and encouragement.

I would like to express my gratitude to Prof. Jayashree Rout, Head, Department of Ecology, Assam University for extending generous help and cooperation.

It's my pleasure to take this opportunity of thanking Dr. Gobinda Das, Dr. Debraj Dhar Purkayastha, Sutapa Chakraborty, Rupam Chakraborty, Nirmalendu Das, Harun All Rashid Pramanik, Rajat Goswami, Dr. Pankaj Goswami, Dr. Sankar Neogi, Abhijit Nath, Bishop Devgupta, Dr. Mridushmita Mishra and Richa Chaturvedi of our group whose help and suggestions always stood by me during the course of my research.

I am grateful to Siddique Anwar for lending me a helping hand in the process of compiling the thesis.

My thanks are due to all the research scholars of the Department, specially Dharitri Das, Sudip Pal and Koushik Barman for their manifold cooperation.

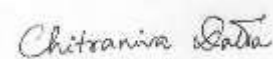
I thank laboratory staffs Mr. P. R. Ramesh, Mr. S. Bhattacharjee, Mr. B. Nath, Mr. A. Barbhuiya and Mr. R. Kurmi. I am thankful to Mr. J. A. Barbhuiya and Mr. L. Hmar, office staffs of the department for their help throughout.

I gratefully acknowledge the cooperation extended by our collaborators, Dr. D. S. S. Rao and Dr. S. K. Prasad, Centre for Nano and Soft Matter Sciences, Bangalore for Powder X-ray Diffraction analysis whenever needed.

I am thankful to SAIF NEHU Shillong, CDRI Lucknow and NEIST Jorhat for providing all spectral facilities.

I thank University Grants Commission (UGC) and Council for Scientific and Industrial Research (CSIR), New Delhi for the financial support.

Words are short to express my deep sense of gratitude and appreciation towards my parents, uncle and aunt whose prayers, love and best wishes were a source of inspiration, encouragement and motivation for me. Without their constant, unwavering and unconditional support nothing would have been possible. My special thanks to my sweet little sister, Paranjaya who always accompanied me in the happy and hard moments.



(Chitraniva Datta)

ABBREVIATIONS

● AcOH	:	Acetic acid
● CHN	:	Carbon, Hydrogen, Nitrogen
● Col	:	Columnar phase
● Col _h	:	Hexagonal columnar phase
● Col _r	:	Rectangular columnar phase
● Col _o	:	Oblique columnar phase
● Col _l	:	Lamello columnar phase
● Col _p	:	Plastic columnar phase
● D	:	Discotic
● d	:	Layer spacing
● dd	:	Doublet of doublets
● DCM	:	Dichloromethane
● DSC	:	Differential Scanning Calorimetry
● DFT	:	Density Functional Theory
● EtOH	:	Ethanol
● FT-IR	:	Fourier transform infra-red
● FAB	:	Fast Atom Bombardment
● I	:	Isotropic
● L	:	Litre
● Ln	:	Lanthanides
● LC	:	Liquid crystal
● M	:	Molarity
● m	:	Multiplet
● MeOH	:	Methanol
● Mpd	:	Methyl phenylene diamine
● MO	:	Molecular orbital
● NMR	:	Nuclear Magnetic Resonance
● N	:	Nematic
● N*	:	Chiral nematic
● opd	:	Ortho phenylene diamine
● ppm	:	Parts per million
● PXRD	:	Powder X-ray Diffraction

● PL	:	Photoluminescence
● POM	:	Polarising Optical Microscope
● rt	:	Room temperature
● s	:	Singlet
● Sm	:	Smectic phase
● t	:	Triplet

LIST OF TABLES

CHAPTERS	TABLES	TITLE	Page No.
CHAPTER 3		: BIDENTATE [N, O]-DONOR SALICYLALDIMINE SCHIFF BASE COMPLEXES OF OXOVANADIUM(IV) AND COPPER(II)	50-74
	Table 1	: UV-visible and photoluminescence data of ligands and complexes	50
	Table 2	: Phase transitions temperatures (T°C), associated enthalpies (ΔH , kJmol ⁻¹) of n-X and their complexes	55
	Table 3	: Selected bond lengths(Å) and bond angles(°) of Cu-6-Cl and Cu-6-NO ₂ complexes optimized at the BLYP/DNP level	60
	Table 4	: Selected bond lengths(Å) and bond angles(°) of VO-6-Cl and VO-6-NO ₂ complexes optimized at the BLYP/DNP level	60
	Table 5	: Spectral data of the compounds	67
	Table 6	: Phase transitions temperatures (T°C), associated enthalpies (ΔH , kJ mol ⁻¹) of the compounds	72
	Table 7	: Selected bond lengths (A°) and bond angles (°C) of VO-6-OC ₁₂ H ₂₅ complex optimized at the BLYP/DNP level of theory	74
CHAPTER 4		: SALOPHEN-BASED TETRADENTATE [N₂O₂]-DONOR SCHIFF BASE COMPLEXES OF OXOVANADIUM(IV), NICKEL(II) AND COPPER(II)	85-113
	Table 1	: UV-visible and photoluminescence data of the compounds	85
	Table 2	: POM and DSC data of the complexes	86
	Table 3	: XRD data of the Ni-16opd	87
	Table 4	: DFT data of the complexes. Bond lengths are reported in Å and bond angles in degrees.	91
	Table 5	: UV-visible data of ligands (n-mpd) and complexes (VO-nmpd)	95

Table 6	:	DSC data of the complexes	97
Table 7	:	XRD data of VO-16mpd	99
Table 8	:	Selected bond length and bond angles of VO-16mpd from DFT study.	101
Table 9	:	UV-visible spectral data of ligands and copper Complexes	104
Table 10	:	Transition temperature ($^{\circ}\text{C}$), enthalpy (kJmol^{-1}) and entropy values (ΔS , $\text{JK}^{-1}\text{mol}^{-1}$) of compounds according to the DSC measurements	108
Table 11	:	XRD data of copper complexes	109
Table 12	:	Selected bond lengths (\AA) and bond angles ($^{\circ}$) and other related parameters of Cu(II) complexes evaluated at B3LYP level.	113
Table 13	:	Natural atomic charges and natural electron configuration of selected atoms of the ligands and their complexes with Cu^{2+} evaluated at B3LYP level.	113
CHAPTER 5	:	HOMODINUCLEAR TRI, [ONO]- AND TETRADENTATE, [N₂O₂]-DONOR SCHIFF BASE COMPLEXES OF COPPER(II) AND ZINC(II)	127-152
Table 1	:	UV-visible and photoluminescence data of Ligands (n-bps) and $\text{Zn}_2\text{-nbps}$ complexes	127
Table 2	:	DSC data of the complexes	130
Table 3	:	Selected bond length and bond angles of $\text{Zn}_2\text{-6bps}$ from DFT	132
Table 4	:	Mesophase transition temperatures (T°C) and associated enthalpies (ΔH , kJ mol^{-1}) of compounds	139
Table 5	:	Selected bond length and bond angles of $\text{Cu}_2\text{L}_2/\text{Cu}_2\text{L}'_2$, from DFT	141
Table 6	:	Thermal data of the Zn_2L_2 complex	145
Table 7	:	XRD data of the Zn_2L_2 complex	146
Table 8	:	Selected bond lengths (\AA) and angles ($^{\circ}$) for the binuclear zinc complex evaluated at B3LYP level	151

Table 9	:	The experimental absorption bands and the electronic transitions calculated with TDDFT/B3LYP method for the ligand.	152
Table 10	:	The experimental absorption bands and the electronic transitions calculated with TDDFT/B3LYP method for binuclear zinc complex	152
CHAPTER 6	:	SALICYLALDIMINE BASED ZWITTERIONIC O-COORDINATED SCHIFF BASE COMPLEXES OF LANTHANIDES(III), (Ln = La, Pr, Sm, Gd, Tb, Dy and Tb)	166-169
Table 1	:	UV-visible data of ligand and lanthanide Complexes	166
Table 2	:	Phase transition temperatures($T^{\circ}\text{C}$), associated enthalpies(ΔH , kJmol^{-1}) of lanthanide complexes	169

LIST OF FIGURES

CHAPTERS	TITLE	Page No.
CHAPTER 1	: GENERAL INTRODUCTION	3-23
Fig. 1	: Some typical examples of Schiff bases of different denticity	3
Fig. 2	: Thermotropic liquid crystalline transition	8
Fig. 3	: Classification of calamitic mesogen	9
Fig. 4	: Molecular order in nematic liquid crystal	9
Fig. 5	: Schematic representation of the molecular ordering in the chiral nematic phase	10
Fig. 6	: Molecular ordering in smectic phases	11
Fig. 7	: General molecular structure of a disc-like liquid crystal	11
Fig. 8	: Classification of discotic mesogen	12
Fig. 9	: a) Discotic nematic phase; b) Chiral nematic phase; c) Nematic columnar phase	13
Fig. 10	: Molecular ordering in hexagonal columnar phase	13
Fig. 11	: Top view of the molecular ordering in the rectangular columnar phase	13
Fig. 12	: Top view of the molecular ordering in the oblique columnar phase	14
Fig. 13	: Molecular ordering in plastic columnar phase	14
Fig. 14	: Molecular ordering in lamello columnar phase	14
Fig. 15	: General structure of bent-core (banana-shaped) liquid crystals	15
Fig. 16	: Structure of lyotropic liquid crystal	16
Fig. 17	: Schiff base-mercury mesogens	18
Fig. 18	: The archetypical salicylaldimine complexes	18
Fig. 19	: Smectic ferrocenyl Schiff bases	19
Fig. 20	: Dithiolene metallomesogen	19
Fig. 21	: Assembly of the diketonate Schiff-base complexes into a discotic antiphase superstructure	20
Fig. 22	: Ligand of the first calamitic lanthanide-containing liquid crystal	21
Fig. 23	: A copper(II) complex of a mesogenic 2,2'-N,N'-bis(salicylidene) ethylenediamine (salen) derivative used to form adducts with lanthanide(III) nitrates	22

Fig. 24	: Simplified Perrin-Jablonski diagram showing the difference between fluorescence and phosphorescence	23
CHAPTER 3	: BIDENTATE [N, O]-DONOR SALICYLALDIMINE SCHIFF BASE COMPLEXES OF OXOVANADIUM(IV) AND COPPER(II)	49-73
Fig. 1	: UV-visible spectra of 4-Cl and 4-NO ₂	49
Fig. 2	: UV-visible spectra of Cu-6-Cl and Cu-6-NO ₂	49
Fig. 3	: UV-visible spectra of VO-6-Cl and VO-6-NO ₂	50
Fig. 4	: Photoluminescence spectra of 4-Cl and 4-NO ₂	50
Fig. 5	: Cyclic voltammogram of Cu-6-NO ₂	51
Fig. 6	: Variation of inverse magnetic susceptibility of VO-6-NO ₂ with temperature	52
Fig. 7	: Fan-like texture of SmA phase(4-Cl)	53
Fig. 8	: DSC thermogram of (4-Cl)	53
Fig. 9	: Schlieren texture of N phase of (6-NO ₂)	54
Fig. 10	: DSC thermogram of 6-NO ₂	54
Fig. 11	: Focal conic texture of SmA phase of (Cu-6-NO ₂)	54
Fig. 12	: DSC trace of Cu-6-NO ₂	55
Fig. 13	: Optimized structure of Cu-6-Cl	57
Fig. 14	: Optimized structure of Cu-6-NO ₂	57
Fig. 15	: Optimized structure of VO-6-Cl	58
Fig. 16	: Optimized structure of VO-6-NO ₂	58
Fig. 17	: HOMO of Cu-6-Cl	58
Fig. 18	: LUMO of Cu-6-Cl	58
Fig. 19	: HOMO of Cu-6-NO ₂	59
Fig. 20	: LUMO of Cu-6-NO ₂	59
Fig. 21	: HOMO of VO-6-Cl complex	59
Fig. 22	: LUMO of VO-6-Cl complex	59
Fig. 23	: HOMO of VO-6-NO ₂ complex	60
Fig. 24	: LUMO of VO-6-NO ₂ complex	60
Fig. 25	: UV-Vis spectra of 4-6-OC ₁₂ H ₂₅ and VO-6-OC ₁₂ H ₂₅	66
Fig. 26	: Variation of magnetic susceptibility of VO-18-OC ₁₂ H ₂₅ with temperature	68
Fig. 27	: Cyclic voltammogram of VO-16-OC ₁₂ H ₂₅	68
Fig. 28	: Schlieren texture of SmC phase	69

Fig. 29	:	DSC thermogram of 4-16-OC ₁₂ H ₂₅	70
Fig. 30	:	Variation of transition temperature with carbon chain length in Ligands	70
Fig. 31	:	Fanlike texture of SmA phase	70
Fig. 32	:	Unidentified SmX phase	71
Fig. 33	:	DSC thermogram of VO-18-OC ₁₂ H ₂₅	71
Fig. 34	:	Variation of transition temperature with carbon chain length in Complexes	71
Fig. 35	:	Optimized structure of VO-6-OC ₁₂ H ₂₅	73
Fig. 36	:	HOMO diagram of VO-6-OC ₁₂ H ₂₅	73
Fig. 37	:	LUMO diagram of VO-6-OC ₁₂ H ₂₅	73
CHAPTER 4	:	SALOPHEN-BASED TETRADENTATE [N₂O₂]-DONOR SCHIFF BASE COMPLEXES OF OXOVANADIUM(IV), NICKEL(II) AND COPPER(II)	84-112
Fig. 1	:	Absorption spectra of the ligands	84
Fig. 2	:	Absorption spectra of the complexes	84
Fig. 3	:	Emission spectra of the Ni-16opd complex	84
Fig. 4	:	POM texture of Ni-16opd complex	86
Fig. 5	:	DSC thermogram of Ni-16opd complex	86
Fig. 6	:	XRD-pattern of Ni-16opd	87
Fig. 7	:	Dimeric interaction of molecules	88
Fig. 8	:	Optimized structure of Ni-16opd	90
Fig. 9	:	LUMO diagram of Ni-16opd	91
Fig. 10	:	HOMO diagram of Ni-16opd	91
Fig. 11	:	UV-vis spectra of 16-mpd and VO-16mpd	94
Fig. 12	:	Cyclic voltammogram of VO-16mpd	95
Fig. 13	:	Combined DSC curve and POM texture of VO-16mpd	97
Fig. 14	:	XRD pattern of VO-16mpd at 40°C	98
Fig. 15	:	XRD pattern of VO-16mpd at 190°C	98
Fig. 16	:	Dimeric interactions of the half disc shaped molecules in the Column	99
Fig. 17	:	Optimized structure of VO-16mpd	100
Fig. 18	:	HOMO of VO-16mpd	101
Fig. 19	:	LUMO of VO-16mpd	101
Fig. 20	:	Absorption spectra of complexes (DCM; 10 ⁻⁵ M)	104
Fig. 21	:	POM texture of Cu-16opd complex at 100°C (20X magnification)	106

Fig. 22	:	DSC thermogram of Cu-16opd complex at 10°Cmin ⁻¹	106
Fig. 23	:	POM texture of Cu-16mpd complex at 152°C	107
Fig. 24	:	DSC thermogram of Cu-16mpd complex at 10°C min ⁻¹	107
Fig. 25	:	XRD pattern of Cu-16opd complex at 130°C	107
Fig. 26	:	XRD pattern of Cu-16mpd complex at 160°C	108
Fig. 27	:	Dimeric interactions of the half disc shaped molecules forming a disc-like shape	108
Fig. 28	:	Optimized structure of Cu-16opd	112
CHAPTER 5	:	HOMODINUCLEAR TRI, [ONO]- AND TETRADENTATE, [N₂O₂]-DONOR SCHIFF BASE COMPLEXES OF COPPER(II) AND ZINC(II)	126-151
Fig. 1	:	UV-visible spectra of 6-bps and Zn ₂ -6bps	126
Fig. 2	:	Emission spectrum of 6-bps in solution and in solid state	127
Fig. 3	:	Emission spectrum of Zn ₂ -6bps in solution and in solid state	127
Fig. 4	:	Schlieren texture of nematic phase (6bps) at 128°C	129
Fig. 5	:	DSC thermogram of 6bps	129
Fig. 6	:	Schlieren texture of SmC (12bps) at 117°C	129
Fig. 7	:	DSC thermogram of (12bps)	130
Fig. 8	:	Optimized structure of Zn ₂ -6bps	131
Fig. 9	:	HOMO of Zn ₂ -6bps	132
Fig. 10	:	LUMO of Zn ₂ -6bps	132
Fig. 11	:	UV-visible spectra of L and Cu ₂ L ₂	136
Fig. 12	:	Emission spectra of ligands in solution and solid state	137
Fig. 13	:	Fanlike texture of SmA phase at 75°C	138
Fig. 14	:	DSC thermogram of L	138
Fig. 15	:	Broken focal conic-shaped texture of SmA at 114°C	139
Fig. 16	:	DSC thermogram of Cu ₂ L ₂	139
Fig. 17	:	Optimized structure of Cu ₂ L ₂	140
Fig. 18	:	Optimized structure of Cu ₂ L ₂	140
Fig. 19	:	UV-visible spectra of the ligand and complex	143
Fig. 20	:	Photoluminescence spectrum of ligand	143
Fig. 21	:	Photoluminescence spectra of zinc complex	144
Fig. 22	:	POM texture of zinc complex	144
Fig. 23	:	DSC thermogram of zinc complex	145
Fig. 24	:	X-ray diffraction pattern of Zn ₂ L ₂ complex at 125°C	146

Fig. 25	:	Molecular organization in discoid shell	146
Fig. 26	:	Optimized structure of binuclear zinc complex	149
Fig. 27	:	Contour plots of some selected molecular orbitals	150
Fig. 28	:	Energy level diagram of MO	151
CHAPTER 6	:	SALICYLALDIMINE BASED ZWITTERIONIC O-COORDINATED SCHIFF BASE COMPLEXES OF LANTHANIDES(III),(Ln = La, Pr, Sm, Gd, Tb, Dy and Tb)	165-168
Fig. 1	:	¹ H NMR spectrum of LH	165
Fig. 2	:	¹ H NMR spectrum of [La(LH) ₃ (NO ₃) ₃]	165
Fig. 3	:	UV-visible spectra of ligand and lanthanide complexes	166
Fig. 4	:	Photoluminescence spectra of the representative compounds	167
Fig. 5	:	Broken fan-like texture of SmA phase of [Dy(LH) ₃ (NO ₃) ₃] complex	168
Fig. 6	:	DSC thermogram of [Dy(LH) ₃ (NO ₃) ₃] complex	168

CONTENTS

Certificate
Declaration
Dedication
Acknowledgement
Abstract
Abbreviations
List of Tables
List of Figures

CHAPTERS	TOPICS	Page No.
CHAPTER 1	GENERAL INTRODUCTION	1-36
	1.1 : Schiff Base	2-3
	1.2 : Schiff base metal complexes	3-4
	1.3 : Structure and properties of some Schiff base metal complexes	4-7
	1.3.1 : Vanadium Schiff base complex chemistry	4-5
	1.3.2 : Nickel Schiff base complex chemistry	5
	1.3.3 : Copper Schiff base complex chemistry	5
	1.3.4 : Zinc Schiff base complex chemistry	6
	1.3.5 : Lanthanide Schiff base complex chemistry	6-7
	1.4 : Application	7-27
	1.4.1 : Liquid Crystal	7-22
	1.4.2 : Photoluminescence	23-25
	1.4.3 : Catalysis	25-26
	1.4.4 : Biological activity	26-27
	1.5 : Objectives	27
	References	28-36
CHAPTER 2	: MATERIALS AND INSTRUMENTAL TECHNIQUES	37-40
	2.1 : Chemicals and solvents	37
	2.2 : Instruments	37-40

CHAPTER 3	: BIDENTATE [N, O]-DONOR SALICYLALDIMINE SCHIFF BASE COMPLEXES OF OXOVANADIUM(IV) AND COPPER(II)	41-78
3.1	: Introduction	42-43
3.2	: Experimental	43-74
	Synthesis of copper (II)/oxovanadium(IV)	
3.2.1	: complexes from bidentate [N,O]-donor polar Schiff base ligands	43-60
3.2.1.1	: Results and discussion	48-60
3.2.2	: Synthesis of oxovanadium(IV) complexes of bidentate [N, O] donor Schiff base ligands	61-74
3.2.2.1	: Results and discussion	65-74
3.3	: Conclusion	75-75
	References	76-78
CHAPTER 4	: SALOPHEN-BASED TETRADENTATE [N₂O₂]-DONOR SCHIFF BASE COMPLEXES OF OXOVANADIUM(IV), NICKEL(II) AND COPPER(II)	79-119
4.1	: Introduction	80-81
4.2	: Experimental	81-113
	Synthesis of mononuclear nickel-salophen complex	
4.2.1	: complex	81-91
4.2.1.1	: Results and discussion	82-91
4.2.2	: Synthesis of oxovanadium(IV) salophen complex	92-101
4.2.2.1	: Results and discussion	93-101
4.2.3	: Synthesis of copper complex with/without substituent in spacer group	101-113
4.2.3.1	: Results and discussion	103-113
4.3	: Conclusion	114-115
	References	116-119
CHAPTER 5	: HOMODINUCLEAR TRI, [ONO]- AND TETRADENTATE, [N₂O₂]-DONOR SCHIFF BASE COMPLEXES OF COPPER(II) AND ZINC(II)	120-157
5.1	: Introduction	121-122
5.2	: Experimental	122-152
	Synthesis of dinuclear zinc complexes bearing tetradentate[N ₂ O ₂] donor of Schiff base ligands	
5.2.1	: complex	122-132

	5.2.1.1	: Results and discussion	125-132
	5.2.2	: Synthesis of dinuclear copper complexes accessed from tridentate [ONO] donor ligands	133-141
	5.2.2.1	: Results and discussion	135-141
	5.2.3	: Synthesis of bimetallic zinc complex from tridentate Schiff base ligand	141-152
	5.2.3.1	: Results and discussion	142-152
	5.3	: Conclusion	152-153
		References	154-157
CHAPTER 6		SALICYLALDIMINE BASED ZWITTERIONIC O-COORDINATED SCHIFF BASE COMPLEXES OF LANTHANIDES(III), (Ln = La, Pr, Sm, Gd, Tb, Dy and Tb)	158-171
	6.1	: Introduction	159-160
	6.2	: Experimental	160-163
	6.2.1	: Synthesis of lanthanide Schiff base complexes	160-163
	6.3	: Results and discussion	163-169
	6.4	: Conclusion	169
		References	170-171
CHAPTER 7		CONCLUSION	172-175

ANNEXURE I : Marksheet of M. Phil. Degree.

ANNEXURE II : Certificate of M. Phil. Degree.

ANNEXURE III : Reprints of published papers.